Non-Markovian theory of activated rate processes. IV. The double well model[a)]

Benny Carmeli and Abraham Nitzan
Department of Chemistry, Tel Aviv University, Faculty of Sciences, Ramat Aviv, 69 978 Tel Aviv, Israel

(Received 19 July 1983; accepted 3 November 1983)

The transition rates associated with a particle moving in a double potential well under the influence of thermal noise and friction is considered as a generalization of Kramers' theory of activated rate processes. We obtain expressions for these transition rates which are valid for all friction and for a general (non-Markovian) interaction between the particle and its thermal environment. Nonthermal equilibrium effects in the steady state distribution in the well as well as effects of trajectories returning unrelaxed from the far wall are explicitly taken into account. The results reduce to all the previously obtained results of the single well model. We use the theory to analyze the experimental results of Hasha, Eguchi, and Jonas.

I. INTRODUCTION

In a recent series of papers[1,2] we have extended Kramers' theory of activated rate[3] processes in two important directions: First[1,2] the low friction limit (where the theory gives a rate proportional to the friction coefficient) was extended to include non-Markovian effects (similar generalizations of the intermediate and high viscosity cases were provided by others).[4,5] Secondly,[3] a method was developed for calculating the steady state rate in the whole friction range, yielding an expression for the rate that reduces to all the Kramers results as well as to their non-Markovian counterparts in the appropriate limits. This general result was obtained for the Kramers (single well) model. In this paper we use the same method to obtain the steady state rates associated with a double well model (Fig. 1) associated with simple isomerization processes. Our results are valid for Markovian as well as for non-Markovian processes.

Several workers have discussed in recent years the double well model for chemical isomerization processes.[6-11] It has long been realized [6,7] that the rate of escape out of a potential well associated with a double well model should be different from that in a single well case because some escaping trajectories may return to their original well after collision with the far wall. This is particularly important for low friction situations; in the high friction limit a trajectory may be safely assumed to relax after crossing the potential barrier before it can return to its original well. Most of the previous studies are restricted to the high friction (diffusion) limit. Others are limited by the use of Markovian dynamics and by the assumption of fast thermal relaxation in the reactant well. The present work removes these restrictions.

There has been in recent years a substantial amount of experimental work on the dependence of the rates of chemical isomerization processes in liquids on the solvent viscosity.[12-15] The present results provide a convenient framework for discussing these experimental results even though the model is obviously oversimplified.

In Sec. II the model is defined and our notation is introduced. The steady state rate is evaluated in the Markovian limit in Sec. III and in the non-Markovian case in Sec. IV. Our results are discussed in relation to other theoretical works and to the experimental observations in Sec. V.

II. THE MODEL

Our starting point is the generalized Langevin equation

$$\ddot{x} = -\frac{1}{M}\frac{dV(x)}{dx} - \int_0^t d\tau\, Z(t-\tau)\dot{x}(\tau) + \frac{1}{M}R(t), \quad (1)$$

$$\langle R(t)\rangle = 0; \quad \langle R(t_1)R(t_2)\rangle = MkTZ(t_1 - t_2), \quad (2)$$

where x is the coordinate of a particle of mass M moving in a potential $V(x)$ under the influence of a thermal force R related to the friction kernel Z by the fluctuation dissipation theorem (2). k is the Boltzmann constant and T the temperature. In the Markovian limit Eqs. (1) and (2) become

$$\ddot{x} = -\frac{1}{M}\frac{dV(x)}{dx} - \gamma\dot{x} + \frac{1}{M}R(t), \quad (3)$$

$$\langle R(t)\rangle = 0; \quad \langle R(t_1)R(t_2)\rangle = 2\gamma MkT\delta(t_1 - t_2), \quad (4)$$

$$\gamma = \int_0^\infty dt\, Z(t). \quad (5)$$

The potential $V(x)$ is displayed in Fig. 1 and is characterized by the barrier energies E_{BL} and E_{BR} with $\Delta E = E_{BL} - E_{BR}$ and by the frequencies characterizing the second derivatives

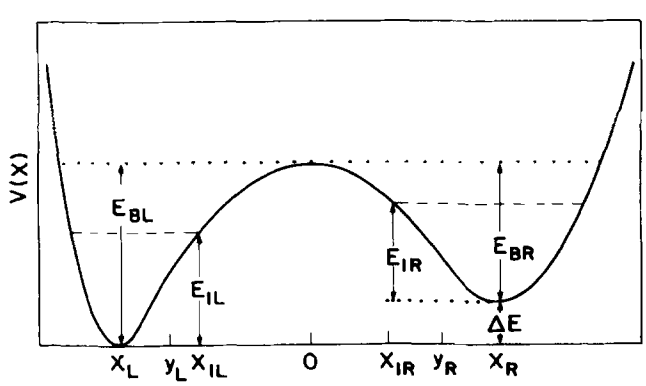

FIG. 1. A schematic representation of the potential used in the present study.

[a)] Supported in part by the Commission for Basic Research of the Israel Academy of Science and by the Binational Science Foundation, Jerusalem, Israel.

 0021-9606/84/083596-10$02.10

of $V(x)$ at the barrier top (ω_B) and at the bottom of the wells (ω_{0L}, ω_{0R}).[16] The indices L and R denote left and right well, respectively.

In what follows we shall use Fokker–Planck equations equivalent to the Langevin equations (1)–(4). In the Markovian limit Eqs. (3) and (4) are equivalent to

$$\frac{\partial P}{\partial t}=\frac{1}{M}\frac{dV}{dx}\frac{\partial P}{\partial v}-v\frac{\partial P}{\partial x}+\gamma\left[\frac{kT}{M}\frac{\partial^2 P}{\partial v^2}+\frac{\partial}{\partial v}(vP)\right], \quad (6)$$

where $P(x,v,t)$ is the probability distribution for the position x and velocity $v=\dot{x}$ of the particle. We shall assume that the wells associated with the potential $V(x)$ are deep ($E_{BR}, E_{BL}\gg kT$) and that far below the barrier top on each side the low friction condition $\gamma\ll\omega$ (ω is the local frequency) is satisfied. In this case the distribution P satisfies

$$P_W(x,v,t)=\frac{M}{2\pi}P_W(J,t), \quad (7)$$

where $P_W(J,t)$ is the distribution function for the action variable J in the well under discussion. The index W (well) denotes that Eq. (7) is valid only deep in the well (the indices L and R will replace W below to denote the left or right wells). $P_W(J,t)$ satisfies the Smulochowski-type equation

$$\frac{\partial P_W}{\partial t}=\gamma\frac{\partial}{\partial J}\left[\frac{J}{\omega(J)}\left(kT\frac{\partial}{\partial J}+\omega(J)\right)P_W\right]. \quad (8)$$

No general result similar to Eq. (6) is available in the non-Markovian case. However near the barrier top, where the potential may be approximated as

$$V(x)=E_{BL}-\frac{M}{2}\omega_B^2 x^2 \quad (9)$$

(measured from the bottom of the left well) the following generalized Fokker–Planck equation for $P(x,v,t)$ holds[5,17]

$$\frac{\partial P}{\partial t}=-\overline{\omega_B^2}\,x\frac{\partial P}{\partial v}-v\frac{\partial P}{\partial x}+\bar{\gamma}\left[\frac{kT}{M}\frac{\partial^2 P}{\partial v^2}+\frac{\partial}{\partial v}(vP)\right]+\frac{kT}{M}\left(\frac{\overline{\omega_B^2}}{\omega_B^2}-1\right)\frac{\partial^2 P}{\partial v\partial x}, \quad (10)$$

where $\bar{\gamma}$ and $\overline{\omega_B^2}$ are functions of time defined by

$$\bar{\gamma}(t)=-\frac{d}{dt}\ln\Phi(t), \quad (11)$$

$$\overline{\omega_B^2}(t)=-\Theta(t)/\Phi(t), \quad (12)$$

$$\Phi(t)=\dot{\rho}(t)\left[1+\omega_B^2\int_0^t d\tau\,\rho(\tau)\right]-\omega_B^2\rho^2(t), \quad (13)$$

$$\Theta(t)=\omega_B^2[\rho(t)\ddot{\rho}(t)-\dot{\rho}^2(t)], \quad (14)$$

$$\rho(t)=\mathcal{L}^{-1}[S^2-\omega_B^2+S\hat{Z}_1-iS)], \quad (15)$$

$$\hat{Z}_1(-iS)=\int_0^\infty dt\,e^{-St}Z(t). \quad (16)$$

$\mathcal{L}^{-1}$ is the inverse Laplace transform. $\bar{\gamma}$ and $\overline{\omega_B^2}$ reduce to the time independent γ and ω_B^2, and Eq. (10) becomes identical to Eq. (6) in the Markovian limit.

The non-Markovian equivalent of Eq. (8) is[1]

$$\frac{\partial P_W}{\partial t}=\frac{\partial}{\partial J}\left\{\epsilon(J)\left[kT\frac{\partial}{\partial J}+\omega(J)\right]P_W\right\}, \quad (17)$$

where

$$\epsilon(J)=2M\sum_{n=1}^{\infty}n^2|X_n(J)|^2\,\mathrm{Re}\{\hat{Z}_n[\omega(J)]\}, \quad (18)$$

$$\hat{Z}_n(\omega)=\int_0^\infty dt e^{-in\omega t}Z(t), \quad (19)$$

and where X_n are the coefficients of the Fourier expansion of the deterministic well motion

$$x=x(J,\varphi)=\sum_{n=-\infty}^{\infty}X_n(J)e^{in\varphi} \quad (20)$$

(φ is the angle variable). In the Markovian limit $\epsilon(J)\to\gamma J/\omega(J)$ and Eq. (17) reduces to Eq. (8).[1]

Equation (17) is still assumed to be valid deep in the well where $P(J,t)$ satisfies Eq. (7). As seen below, our results hold also if the range of validity of Eqs. (7), (8), or (17) shrinks to zero.

The situation of interest for the present work is as follows: At time $t=0$ the particles occupy one (say the left for definiteness) well and the process starts. After some incubation period we get a quasi-steady-state situation, characterized by an almost constant net flux of particles from left to right. The condition $E_B\gg kT$ insures the time scale separation necessary for the steady state concept to be meaningful.

It is mathematically convenient, and of no physical consequence, to make the steady state situation precise by imposing particle sources/sinks near the bottom of the wells. Their function is the same on both sides: to keep fixed total numbers of particles below certain energies E_{0L} and E_{0R} in the left and right wells. The extreme case described above corresponds to an absorbing boundary at E_{0R} and to a source keeping a Boltzmann distribution with a constant total number of particles below E_{0L}. This constant number corresponds to the equilibrium population that would have existed in the absence of the barrier crossing process. These mathematical boundaries just make precise a situation which prevails to an excellent approximation also in their absence. It is intuitively clear and will be indeed seen that the final result for the rate should not depend on the exact values of E_{0L} and E_{0R} as long as they are located close enough to the bottoms.[18]

III. STEADY STATE SOLUTION IN THE MARKOVIAN CASE

As in previous work[2] we first write separately the steady state solutions near the barrier top and in the wells and then combine them together in a way which satisfies essential continuity requirement.

A. Solution in the wells

The boundary conditions implied by the presence of source/sink near the well bottoms are expressed by

$$P_L(J)=A_{0L}\exp[-E_L(J)/kT], \quad 0\leqslant J\leqslant J_{0L}, \quad (21)$$

$$P_R(J)=A_{0R}\exp[-E_R(J)/kT], \quad 0\leqslant J\leqslant J_{0R}, \quad (22)$$

where $P_L(J)$ and $P_R(J)$ correspond to the left and right wells, respectively, $E_W(J)$ ($W=L,R$) are the energies measured from the bottom of the corresponding wells [note that E_L

may be a different function of J than E_R is; generally

$$E_W(J) = \int^J dJ'\omega_W(J')$$

and the functions $\omega(J)$ are in principle different in the two wells]. J_{0L} and J_{0R} are the actions associated with the energies E_{0L} and E_{0R} defined in the previous section.

Between E_0 and some $E_1(>E_0)$ we assume that Eq. (8) is valid. A general steady-state solution is

$$P_W(J) = A_W \exp\left[-\frac{E_W(J)}{kT}\right] \times\left\{B_W + \int_J^{J_{1W}} dJ' \frac{\omega_W(J')}{\gamma J'} \exp\left[\frac{E_W(J')}{kT}\right]\right\}, \quad J_{0W}\leqslant J\leqslant J_{1W} \tag{23}$$

with $W = L, R$. The requirement that $P_W(J_0)$ is the same when calculated from Eq. (21) or (23) implies that

$$A_{0W} = A_W\left\{B_W + \int_{J_{0W}}^{J_{1W}} dJ \frac{\omega_W(J)}{\gamma J} \times \exp[E_W(J)/kT]\right\} \quad (W = L, R). \tag{24}$$

The steady state currents associated with the distributions $P_L(J)$ and $P_R(J)$ are obtained from

$$j_W = -\gamma \frac{J}{\omega_W(J)}\left[kT\frac{d}{dJ} + \omega_W(J)\right]P_W(J), \tag{25}$$

which yield

$$j_W = A_W kT. \tag{26}$$

Note that Eq. (25) gives the probability current in the direction of increasing J. The actual directions of j_L and j_R are determined by the signs of A_L and A_R. Also note that the role of the source/sink agents at J_{0L} and J_{0R} is to absorb these currents so that no currents exist below J_{0L} and J_{0R} in the corresponding wells as indeed implied by Eqs. (21) and (22).

B. Solution near the barrier top

Here the Kramers procedure[1] may be followed leading to the steady state distribution

$$P_B(x, v) = F_2 \exp\left\{-\left[\frac{M}{2}v^2 + V(x)\right]/kT\right\} \times\left[F_1 + \int_0^{v-\gamma(\alpha+1)x} dz \exp\left(-\frac{\alpha M z^2}{2kT}\right)\right], \tag{27}$$

where

$$\alpha = \sqrt{\tfrac{1}{4} + (\omega_B/\gamma)^2} - \tfrac{1}{2}. \tag{28}$$

The current associated with $P_B(x, v)$ is calculated from $j_B = \int_{-\infty}^{\infty} dv\, vP_B(x,v)$. The result is

$$j_B = F_2\left(\frac{kT}{M}\right)^{3/2}\sqrt{\frac{2\pi}{\alpha+1}}\exp\left(-\frac{E_{BL}}{kT}\right). \tag{29}$$

Note that a positive j_B describes a current in the positive x direction (from left to right). The actual direction depends on the sign of F_2.

The expressions obtained above for the probability distribution in different sections of the system are characterized by eight parameters: A_L, A_R, B_L, B_R, F_1, F_2, E_{1L}, and E_{1R}. These are determined below so as to affect smooth transitions between the different expressions.

C. Parameter determination

To determine the eight parameters listed above we apply the following continuity requirements[2]:

(a) Continuity of the distribution at the points $(E_{1L}, v = 0)$ and $(E_{1R}, v = 0)$. Using Eq. (7) this yields for the left well

$$\frac{M}{2\pi}P_L(J_{1L}) = P_B(X_{1L}, v = 0) \tag{30}$$

and similarly for the right well

$$\frac{M}{2\pi}P_R(J_{1R}) = P_B(X_{1R}, v = 0). \tag{31}$$

In Eqs. (30) and (31) J_{1W} and X_{1W} $(W = L, R)$ are related to the energy E_{1W} by

$$E_{1W} = \int_0^{J_{1W}} \omega_W(J)\, dJ \tag{32}$$

and

$$X_{1W} = \pm\frac{1}{\omega_B}\sqrt{\frac{2(E_{BW} - E_{1W})}{M}}. \tag{33}$$

In Eq. (33) the positive sign is for $W = R$ and the negative for $W = L$.

(b) Continuity of the derivatives (with respect to energy) of the probability distribution taken with $v = 0$ at E_{1L} and E_{1R}:

$$\left[\frac{\partial}{\partial E}P_B(x, v = 0)\right]_{E_{1W}} = \left[\frac{\partial}{\partial E}P_W(E)\right]_{E_{1W}}. \tag{34}$$

Using Eqs. (32) and (33) this leads to

$$\frac{\left[\frac{\partial}{\partial x}P_B(x, v = 0)\right]_{X_{1L}}}{\omega_B\sqrt{2M(E_{BL} - E_{1L})}} = \frac{\left[\frac{\partial}{\partial J}P_L(J)\right]_{J_{1L}}}{\omega_L(J_{1L})} \tag{35}$$

and

$$\frac{-\left[\frac{\partial}{\partial x}P_B(x, v = 0)\right]_{X_{1L}}}{\omega_B\sqrt{2M(E_{BR} - E_{1R})}} = \frac{\left[\frac{\partial}{\partial J}P_R(J)\right]_{J_{1R}}}{\omega_R(J_{1R})}. \tag{36}$$

(c) Equality of currents, namely

$$j_B = j_L = -j_R, \tag{37}$$

Eqs. (30), (31), and (35)–(37) provide six continuity conditions. The rational behind them is discussed elsewhere.[2] In addition the ratio

$$q_0 = \frac{A_{0L}\omega_{0L}}{A_{0R}\omega_{0R}} \tag{38}$$

is assumed to be given. This is the ratio between the populations of the left and right wells that is obtained if an infinite barrier is imposed between them.[19] To a good approximation this remains the population ratio in the steady state established after this barrier is removed to allow the beginning of the process.

Since ω_{0L} and ω_{0R}, the frequencies at the bottom of the potential wells, are known, a knowledge of q_0 gives with Eq.

(24) an additional relation between A_{1L}, B_{1L}, A_{1R}, and B_{1R}. The last necessary condition is normalization: the net rate r is defined as the normalized current

$$r = j/N, \tag{39}$$

where

$$N = \int_{-\infty}^{\infty} dv \int_{-\infty}^{\infty} dx\, P(x,v) \tag{40}$$

and thus contains no free parameters.

Carrying out the procedure described above involves calculations and approximations similar to those done in previous work.[2] For the sake of completeness the essential points are given in Appendix A. The final result is

$$r = \frac{q_s - q_e}{q_s + 1}\left[\tau_L + q_e\tau_R + \tfrac{1}{2}(\bar{S}_L + \bar{S}_R)r_{K,RL}^{-1}\right]^{-1}, \tag{41}$$

where

$$q_s = N_L/N_R \tag{42}$$

is the steady-state population ratio (N_L and N_R are defined by Eqs. (A18) and (A19) and are given by Eqs. (A20) and (A21).

$$q_e = \frac{Q_L}{Q_R} e^{\Delta E/kT} \tag{43}$$

is the equilibrium population ratio [Q_L and Q_R are the wells partition functions defined in Eqs. (A14) and (A15)]:

$$\tau_W = \frac{1}{kT}\int_{J_{0W}}^{J_{1W}} dJ \frac{\omega_W(J)}{\gamma J} \exp\left[\frac{E_W(J)}{kT}\right] \int_0^J dJ' \times \exp\left[-\frac{E_W(J')}{kT}\right] \quad (W = L, R) \tag{44}$$

are the mean first passage times to reach J_{1W} starting from J_{0W}, given reflective barriers at $J = 0$ in the corresponding right ($W = R$) or left ($W = L$) wells,

$$r_{K,RL} = \frac{\omega_{0L}}{2\pi\omega_B}\left(\sqrt{\left(\frac{\gamma}{2}\right)^2 + \omega_B^2} - \frac{\gamma}{2}\right)\exp\left(-\frac{E_{BL}}{kT}\right) \tag{45}$$

is the Kramers' left to right rate for a single well model in the intermediate to high friction range, and finally [with R_W defined by Eq. (A7)]

$$\bar{S}_W = \frac{\int_0^{E_{BW}} \frac{dE}{\omega_W(E)}[\eta(E - E_{1W}) + R_W\eta(E_{1W} - E)]\exp\left(-\frac{E}{kT}\right)}{\int_0^{E_{BW}} \frac{dE}{\omega_W(E)}\exp\left(-\frac{E}{kT}\right)}, \tag{46}$$

where $\eta(x) = 0$ for $x < 0$ and $\eta(x) = 1$ for $x > 0$. The matching point energies E_{1W} ($W = L,R$) are obtained as the solutions of Eq. (A9).

The rate r, Eq. (41) corresponds to the net flux (defined to be positive for net flux going from left to right). The transition rates from the left to the right well (r_{RL}) and from the right to left well (r_{LR}) are obtained as the $q_s \to \infty$ and $q_s \to 0$ limits, respectively,

$$r_{RL} = r(q_s \to \infty) = \left[\tau_L + q_e\tau_R + \tfrac{1}{2}(\bar{S}_L + \bar{S}_R)r_{K,RL}^{-1}\right]^{-1}, \tag{47}$$

$$r_{LR} = r(q_s \to 0) = \left[\frac{1}{q_e}\tau_L + \tau_R + \tfrac{1}{2}(\bar{S}_L + \bar{S}_R)r_{K,LR}^{-1}\right]^{-1}, \tag{48}$$

where $r_{K,LR}$ the right to left Kramers' single well rate is obtained from Eq. (45) by replacing ω_{0L} and E_{BL} by ω_{0R} and E_{BR} in Eq. (45). Note that these rates satisfy the detailed balance requirement

$$r_{LR}/r_{RL} = q_e. \tag{49}$$

Also note that the total current $r(N_L + N_R)$ may be written [using Eqs. (41), (43), and (49)] as $N_L r_{RL} - N_R r_{LR}$ thus exhibiting the usual chemical kinetics behavior.

IV. STEADY STATE SOLUTION IN THE NON-MARKOVIAN CASE

As discussed in previous works,[2,5] the steady state escape rate associated with the non-Markovian model, Eqs. (1) and (2) may be derived in exact analogy to the Markovian case using Eqs. (10) and (17) (with $\partial P/\partial t = 0$) as starting points for the corresponding barrier and well regions. The formal forms of the results (41), (47), and (48) remain the same and the following changes enter in the definitions of the parameters τ_W ($W = L, R$) and $r_{K,RL}$:

(a) τ_L and τ_R are given by equations similar to Eq. (44) with $\gamma J/\omega_W(J)$ replaced by $\epsilon_W(J)$ [Eq. (18)]. Thus,

$$\tau_W = \frac{1}{kT}\int_{J_{0W}}^{J_{1W}} \frac{dJ}{\epsilon_W(J)} \exp\left[\frac{E_W(J)}{kT}\right] \times \int_0^J dJ' \exp\left[-\frac{E_W(J)}{kT}\right]. \tag{50}$$

(b) The joining points E_{1W} and the corresponding x_{1W}, J_{1W} ($W = L, R$) are given by equations similar in form to Eq. (A9), again with the replacement of $\gamma J/\omega_W(J)$ by $\epsilon_W(J)$,

$$\exp\left(-\bar{\alpha}\frac{E_B - E_{1W}}{kT}\right) = \sqrt{\bar{\alpha}\frac{E_B - E_{1W}}{kT}}\,\frac{kT}{\epsilon_W(J_{1W})\omega_W(J_{1W})\sqrt{\pi(\bar{\alpha}+1)}} \tag{51}$$

and with $\bar{\alpha}$ defined by

$$\bar{\alpha} = \frac{\omega_B^2}{\Gamma^2 - \omega_B^2} \tag{52}$$

$$\Gamma = -\lim_{t\to\infty}\left[\frac{\bar{\gamma}(t)}{2} + \sqrt{\left(\frac{\bar{\gamma}(t)}{2}\right)^2 + \overline{\omega_B^2}(t)}\right]\frac{\omega_B^2}{\overline{\omega_B^2}(t)}, \tag{53}$$

where $\bar{\gamma}(t)$ and $\overline{\omega_B^2}(t)$ are defined by Eqs. (11) and (12). It is easy to show that $\bar{\alpha}$ reduces to α [Eq. (28)] in the Markovian limit.

(c) The Kramers rates $r_{K,RL}$ and $r_{K,LR}$ are given by equations similar to Eqs. (A32) and (A36),

$$r_{K,RL} = \frac{\omega_{0L}}{2\pi\omega_B}\lambda_0 \exp\left(-\frac{E_{BL}}{kT}\right), \tag{54a}$$

$$r_{K,LR} = \frac{\omega_{0R}}{2\pi\omega_B}\lambda_0 \exp\left(-\frac{E_{BR}}{kT}\right), \tag{54b}$$

$$\lambda_0 = \lim_{t\to\infty}\left\{\sqrt{\left[\frac{\bar{\gamma}(t)}{2}\right]^2 + \overline{\omega_B^2}(t)} - \frac{\bar{\gamma}(t)}{2}\right\}. \tag{55}$$

λ_0 may be calculated[2,4,5] as the largest (real and positive) root of the equation

$$\lambda^2 - \omega_B^2 + \lambda\hat{Z}_1(-i\lambda) = 0, \tag{56}$$

where $\hat{Z}_1$ is defined by Eq. (19).

Equations (41), (47), and (48) with the parameters defined above provide readily calculable expressions for the rates associated with the non-Markovian double well problem.

V. DISCUSSION

For definiteness we focus our discussion on r_{RL}, the steady state transition rate from the left to the right well given by

$$r_{RL} = [\tau_L + q_e\tau_R + \tfrac{1}{2}(\bar{S}_L + \bar{S}_R)r_{K,RL}^{-1}]^{-1}, \tag{57}$$

where τ_L and τ_R are given by Eq. (44) in the Markovian limit and by Eq. (50) for the non-Markovian case, and are identified as the mean first passage times to reach E_{1W} starting from E_{0W} ($W = L, R$) in the stochastic motion governed by Eqs. (8) (Markovian) or (17) (non-Markovian), given a reflecting barrier at $E = 0$; $r_{K,RL}$ is given by Eqs. (45) (Markovian) or (54)–(56) (non-Markovian) and is the Kramers single well escape rate; S_L and S_R are parameters defined by Eq. (46). The joining points energies E_{1L} and E_{1R} which appear in τ_L, τ_R, $\bar{S}_L$, and $\bar{S}_R$ are determined by the continuity conditions and are given by Eqs. (A9) (Markovian) or (51) (non-Markovian). In the Markovian case it is easy to show that the solutions E_{1W} to these equations are monotonically decreasing functions of the friction γ and that $E_{1W}\to E_{BW}$ for $\gamma\to 0$ while $E_{1W}\to 0$ for $\gamma\to\infty$. The latter holds also in the non-Markovian case [where γ is defined by Eq. (5)].

For large friction, $\gamma\to\infty$, τ_L and τ_R in Eq. (57) decrease (since E_{1L} and E_{1R} do). At the same time $\bar{S}_L$ and $\bar{S}_R$ become unity so

$$r_{RL}\to r_{K,RL} \quad (\gamma\to\infty). \tag{58}$$

This implies, as is intuitively expected, that for large friction the double well nature of the potential surface does not affect the escape rate: a trajectory which passes from left to right will relax in the right well before bouncing off the far right wall.

The situation is quite different in the low friction limit. In this case $E_{1R}\to E_{BR}$ and $E_{1L}\to E_{BL}$, thus $\bar{S}_R, \bar{S}_L\to 0$ and

$$r_{RL}\to\frac{1}{\tau_L + q_e\tau_R}, \tag{59}$$

where τ_L and τ_R are given by Eqs. (44) or (50) with E_{BW} replacing E_{1W}. This result should be compared to the single well result in this limit $r\to\tau_L^{-1}$. The additional term, $q_e\tau_R$, in the denominator of Eq. (59) represents the effect of the back scattering of trajectories from the far wall by the product well.

The following points should be made concerning these results:

(a) Even though τ_L and τ_R appear to depend on the (arbitrary) choice of E_{0L} and E_{0R} [cf. Eqs. (44) and (50)] there is actually no dependence on these parameters provided that $E_{1W} \gg E_{0W}$ ($W = L, R$). In cases for which τ_L and τ_R are not negligible in Eq. (57) relative to the $r_{K,RL}^{-1}$ term, E_{1W} is of the order of E_{BW}, thus E_{0W} should be of order kT or less. A further discussion of this point is provided in Ref. 2.

(b) A common approximation to the mean first passage times τ_L and τ_R to reach the points E_{1L} and E_{1R} is given by the Kramers' expression[20]

$$\tau_W \simeq \frac{kT}{\omega_{0W}\gamma J_{1W}}\exp\left(\frac{E_{1W}}{kT}\right) \quad \text{(Markovian)} \tag{60}$$

or its non-Markovian analog

$$\tau_W \simeq \frac{kT}{\omega_{0W}\epsilon_W(J_{1W})\omega_W(J_{1W})} \times \exp\left(\frac{E_{1W}}{kT}\right) \quad \text{(non-Markovian)}. \tag{61}$$

It may be shown[1,4(c)] that the result (61) becomes identical to result (60) for $E_{1W}/kT\to\infty$. These results show again that the choice of E_0 is of no consequence and also provide quick estimates for an approximate evaluation of r_{RL} [Eq. (57)].

(c) The result (59) shows that under weak friction conditions the double well nature of the potential has a considerable influence on the transition rate. This is due to collisions of escaping trajectories with the far wall which causes them to return to their original well. In fact, in the symmetric case ($\tau_L = \tau_R$, $q_e = 1$) the rate (59) is half of the value (τ_L^{-1}) associated with the $\gamma\to 0$ limit of the single well model. This corresponds to a picture where an escaping trajectory goes through a relatively long period of oscillations between the two far walls and has equal (for the symmetric case) probabilities of ending in either well.

Our results (59) and (57) give a simple expression of the transition rate which includes the effect of this backscattering process and, more generally, accounts for the competition between the barrier dynamics which lead to transitions from well to well and between the energy relaxation (and accumulation) processes in the wells.

(d) The general expression (57) yields the correct single well expression when we take $E_{BR}\to\infty$ (i.e., taking the bottom energy of the right well to $-\infty$). In this case $q_e\to 0$ while both E_{BR}/kT and $(E_{BR} - E_{1R})/kT$ become large, implying $R_R\to 1$ and $S_R\to 1$ in Eq. (46). Thus we get

$$r_{RL}\to[\tau_L + \tfrac{1}{2}(\bar{S}_L + 1)r_{K,RL}^{-1}]^{-1}$$

which is the single well result for both the Markovian and the non-Markovian cases.[2,21]

There are several previous works on the escape problem within the double well model. Most of these focus on the diffusion (high friction) limit. Of particular relevance to our discussion are the works of Chandler[6(a)] and of Montgomery,

Chandler, and Berne[6(b)] and the work of Northrup and Hynes.[7] The numerical calculation of Montgomery, Chandler, and Berne[6(b)] (based on the work of Chandler[6(a)]) is based on a thermal equilibrium picture in which trajectories sampled from a Maxwell Boltzmann distribution are started on the barrier. This calculation yields a rate which becomes proportional to the friction[22] for small friction due to the backscattering effect discussed above. However due to its underlying equilibrium nature it cannot account for the other effect which leads to a rate proportional to γ even in the single well model—the deviation from equilibrium in the reactant well which occurs in the small friction steady state situation. Our result takes both effects into account by the appearance of the terms τ_L and $q_e\tau_R$ in Eq. (57) (see also discussion below).

Even though the calculation of Northrup and Hynes (NH)[7(a)] is done in the diffusion (high friction) limit, their result bears a remarkable resemblance to our more general expression (57). To see this consider their result [Ref. 7(a), Eq. (4.4)] in our notation:

$$r_{RL} = \frac{k_{RL}}{1 + (k_{RL}/k_L) + (k_{LR}/k_L)}, \tag{62}$$

where k_{RL} and k_{LR} are the "barrier rate constants" to go from left to right and from right to left, respectively, while k_L and k_R are rates for internal relaxation in the left and right wells. Rewriting Eq. (62) in the form

$$r_{RL} = \left[k_L^{-1} + \left(\frac{k_{LR}}{k_{RL}}\right)k_R^{-1} + k_{RL}^{-1}\right]^{-1} \tag{63}$$

and noting that k_{LR}/k_{RL} is equal to the ratio q_e between the equilibrium populations of the left and right wells, we see that Eq. (63) is similar to Eq. (57) where τ_L, τ_R, and $r_{K,RL}^{-1}$ are equivalent to k_L^{-1}, k_R^{-1}, and k_{RL}^{-1}, respectively (note that in the high fraction limit taken by NH, $\bar{S}_L = \bar{S}_R = 1$).

This remarkable resemblance exists despite the fact that the rates k_L and k_R are related to motion on the coordinate axis while τ_L^{-1} and τ_R^{-1} are rates associated with energy accumulation and relaxation. The reason is that Eqs. (57) and (62) have the general form of an overall rate associated with consecutive rate processes. To see this consider the simple kinetic scheme $L \underset{k_{LI}}{\overset{k_{IL}}{\rightleftarrows}} I \underset{k_{IR}}{\overset{k_{RI}}{\rightleftarrows}} R$ with the time evolution given by

$$\frac{dL}{dt} = -k_{IL}L + k_{LI}I, \tag{64a}$$

$$\frac{dI}{dt} = k_{IL}L - (k_{LI} + k_{RI})I + k_{IR}R, \tag{64b}$$

$$\frac{dR}{dt} = k_{RI}I - k_{IR}R. \tag{64c}$$

In a steady state determined by $R = 0$, $L = \text{const}$ and $dI/dt = 0$ [so that additional source and sink terms are needed in Eqs. (64a) and (64c) respectively], Eq. (64b) yields $I = k_{IL}k_{RI}(k_{LI} + k_{RI})^{-1}$ and the steady state rate of product formation is obtained from $(dR/dt)_{ss} = k_{RI}(I)_{ss}$ to be

$$\left(\frac{dR}{dt}\right)_{ss} = \left(\frac{k_{LI}}{k_{IL}}k_{RI}^{-1} + k_{IL}^{-1}\right)^{-1}$$
$$= \left[\left(\frac{L}{I}\right)_{eq}\left(\frac{I}{R}\right)_{eq}k_{IR}^{-1} + k_{IL}^{-1}\right]^{-1}$$
$$= \left[\left(\frac{L}{R}\right)_{eq}k_{IR}^{-1} + k_{IL}^{-1}\right]^{-1}$$

which is similar to our low friction limit result (59) if we identify τ_L with k_{IL}^{-1}, τ_R with k_{IR}^{-1}, and $(L/R)_{eq}$ with q_e. The NH result is thus an analog of Eq. (57) where the consecutive rate processes all occur in the diffusion limit. In fact, in their later work[7(b)] Northrup and Hynes provides a derivation of Eq. (62) based on a multistep master equation model which is not limited to the diffusion limit. It should be noticed that in the NH approach the location of the "stable state surface" which separates between the well and the barrier regions has to be determined by additional assumptions while here it is obtained as part of the solution.

In order to study in more detail the actual predictions of our double well model and to test their dependence on the different parameters we have employed a potential similar to that used by Montgomery, Chandler, and Berne[6(b)]

$$V(x) = \begin{cases} \frac{M}{2}\omega_{0L}^2(x - X_L)^2, & x < Y_L, \\ E_B - \frac{M}{2}\omega_B^2 x^2, & Y_L < x < Y_R, \\ \Delta E + \frac{M}{2}\omega_{0R}^2(x - X_R)^2, & Y_R < x. \end{cases} \tag{65}$$

This potential is displayed schematically in Fig. 1 where the parameters appearing in Eq. (65) are also shown. Y_L and Y_R are determined so as to affect continuity in the potential and its x derivative. These requirements lead to the relations

$$Y_W = \frac{X_W\omega_{0W}^2}{\omega_{0W}^2 + \omega_B^2} \quad (W = L, R) \tag{66}$$

$$= \frac{2(\omega_{0L}^2 + \omega_B^2)E_{BL}}{\omega_{0L}^2\omega_B^2 X_L^2} = \frac{2(\omega_{0L}^2 + \omega_B^2)E_{BR}}{\omega_{0R}^2\omega_B^2 X_R^2}, \tag{67}$$

$$\Delta E = E_{BL}\left[1 - \frac{(\omega_{0L}^2 + \omega_B^2)\omega_{0R}^2 X_R^2}{(\omega_{0R}^2 + \omega_B^2)\omega_{0L}^2 X_L^2}\right] \tag{68}$$

leaving free the choice of six parameters, e.g., E_B, ω_B, ω_{0L}, ω_{0R}, X_L, and X_R.

In Fig. 2 we show the transmission coefficient r/r_{TST} as a function of friction for a range of parameters which determine the shape of the potential and the time scale associated with the motion of the thermal bath. E_B was taken to be 10.7 kcal/mol (corresponding to the activation energy of cyclohexane[13]). The rate r is obtained from Eq. (57) and for the function $Z(t)$ [Eq. (2)] we have used

$$Z(t) = \frac{\gamma}{\tau_c}\exp\left(-\frac{t}{\tau_c}\right) \tag{69}$$

implying

$$\hat{Z}_n(\omega) = \frac{\gamma}{1 + i\eta\omega\tau_c}. \tag{70}$$

In the results reported below we use a symmetric double well

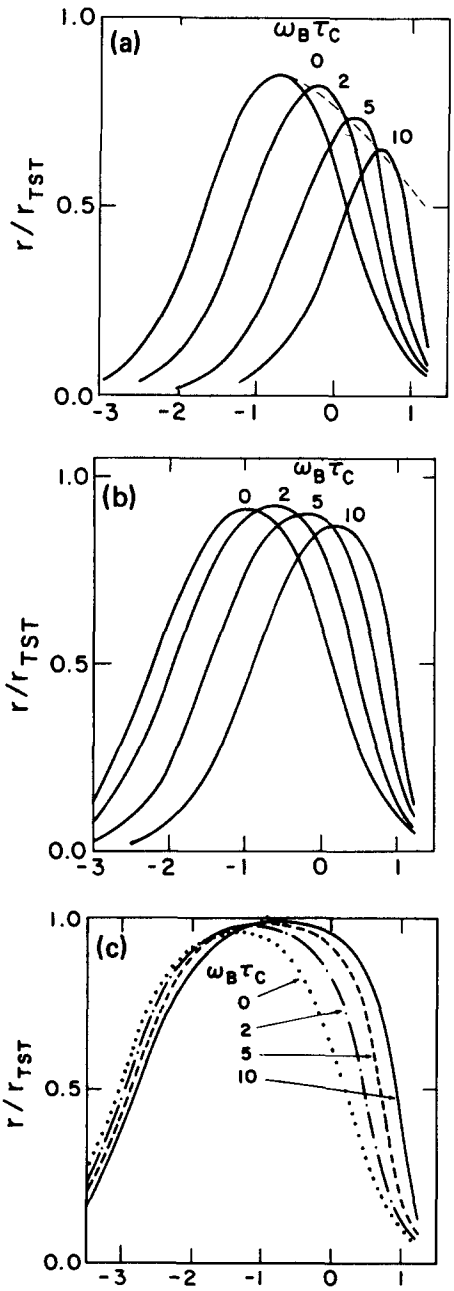

FIG. 2. The transmission coefficient r/r_{TST} as a function of γ/ω_B for a symmetric double well potential with $E_B = 10.7$ kcal/mol. ($\simeq 18kT$ for $T = 300$ K) (a) $\omega_0/\omega_B = 5$; (b) $\omega_0/\omega_B = 1$; (c) $\omega_0/\omega_B = 0.2$. The dashed line in Fig. 2(a) illustrates the weaker dependence of the rate on γ obtained if τ_c is taken to increase with γ.

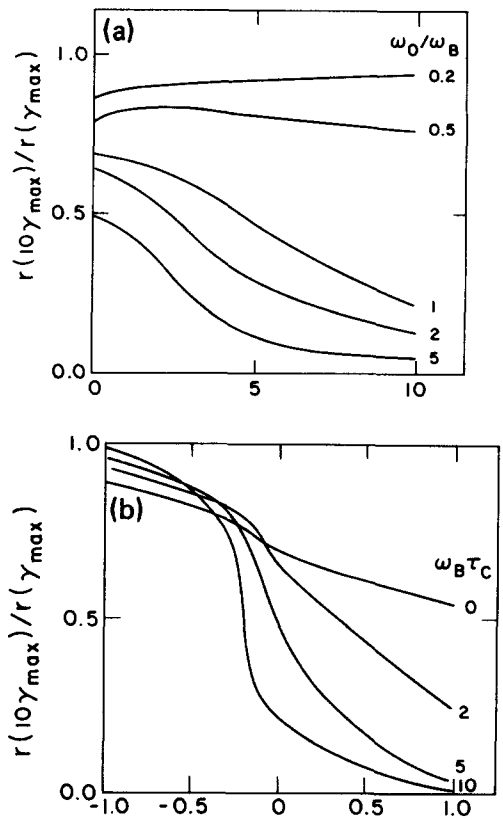

FIG. 3. $r(10\gamma_{max})/r(\gamma_{max})$ as a function of $\omega_B\tau_C$ [Fig. 3(a)] and of ω_0/ω_B [Fig. 3(b)] for a symmetric double well potential with $E_B = 10.7$ kcal/mol.

potential and denote $\omega_0 \equiv \omega_{0R} = \omega_{0L}$. Figures 2(a)–2(c) correspond respectively to $\omega_0/\omega_B = 5$, 1, and 0.2. In each figure the different curves correspond to values of $\omega_B\tau_c$ ranging from 0 to 10. In Fig. 3 we focus on one particular feature of the friction dependence of the rate. Denoting γ_{max} this value of γ [of Eqs. (69) and (70)] for which r/r_{TST} is maximum we plot $r(10\gamma_{max})/r(\gamma_{max})$ as a function of $\omega_B\tau_c$ [Fig. 3(a)] and of ω_0/ω_B [Fig. 3(b)]. The magnitude of $r(10\gamma_{max})/r(\gamma_{max})$ corresponds to the change in the rate as γ increases by an order of magnitude beyond its maximal rate value. This is the friction range considered in the cyclohexane isomerization rate experiments of Hasha, Eguchi, and Jonas.[13] These authors have observed a dependence of the rate on viscosity which is qualitatively similar to that depicted in Fig. 2. For $\eta > \eta_{max}$ (η being the viscosity and η_{max} correspond to the maximal transmission coefficient) they report a slow decrease in the rate with increasing viscosity: r/r_{TST} decreases by about 2%–10% (depending on the assumed value of the TST activation volume) in the range $\eta = \eta_{max} \cdots 10\eta_{max}$.

These results as well as other experimental observations of a relatively slow decrease in the transmission coefficient for increasing viscosity[5(b),12] have been attributed by Velsko, Waldeck, and Fleming,[12(b)] by Bagchi and Oxtoby,[24] and by Hanggi and Mojtabai[5(b)] to non-Markovian effects in the barrier dynamics. On the other hand, Garrity and Skinner[9] have argued that the results of Hasha *et al.*[13] may be rationalized within the Markovian limit as resulting from a potential with relatively narrow wells and a very wide barrier.[25] The results displayed in Figs. 2 and 3 indicate that the situation is far more complicated.

It should first be pointed out that our numerical results are in qualitative agreement with those obtained by Garrity and Skinner,[9] however we do not agree with their interpretation. These authors observe (see Fig. 3 of Ref. 9) that the wider the barrier the larger is the (downwards) deviation of the maximum steady state rate from the TST result. This is to be expected since for a wider barrier the friction plays a more important role in reducing the rate relative to the TST value. Then, since the rate vanishes for both $\gamma \to 0$ and $\gamma \to \infty$ it follows that the rate goes to zero with increasing γ more slowly for wider barriers, in apparent agreement with the observations of Ref. 13.

This is however an "optical illusion." To make a proper comparison with Fig. 9 of Ref. 13 one has to follow Hasha *et al.*[13] in scaling the rate with respect to its maximum value and in looking at the friction dependence in a range of about one order of magnitude beyond its maximal rate value γ_{max}. In contrast to this, in Fig. 3 of Ref. 9 the curve with $bX_0 = 9$ is shown only in the range $\gamma_{max} \cdots 1.6\gamma_{max}$ (on the high friction side).

When this is done (Figs. 2 and 3) we reach a conclusion opposite to that of Garrity and Skinner: It is for barriers of higher curvature (larger ω_B) that we get a better agreement with the experimental result. This is most clearly seen in Fig. 3(a) where the values of $r(10\gamma_{max})/r(\gamma_{max})$ are in good agreement with observation for $\omega_0/\omega_B = 0.2$.

This dependence on ω_B is in agreement with the suggestion of Bagchi and Oxtoby[24] and of Velsko *et al.*[12(b)] that the relatively weak dependence of r on the viscosity is associated with non-Markovian barrier dynamics. Indeed for larger ω_B this effect should be stronger. Inspection of the results of Figs. 2 and 3 reveals however that the situation is less simple. It is seen from these figures that the dependence of the rate on the friction strongly depends on the ratio ω_0/ω_B in a way that cannot be described by considering barrier dynamics alone [i.e., Eqs. (54)–(56)]. In fact the experimental results of Hasha *et al.*[13] can be fitted by adjusting ω_0/ω_B. This is shown in Fig. 4 where these results (corresponding to $\Delta V^{\neq}_{TST} = -1.5$ cm^3/mol) are shown together with our theoretical curves for $\omega_0/\omega_B = 0.2$ and $\omega_B\tau_c = 0$ and 10. Obviously, for some $\omega_B\tau_c$ between 0 (Markovian case) and 10 an excellent agreement will be obtained. It should however be pointed out that the experimental results may be shifted towards either of the theoretical curves shown using a different (but equally reasonable) guess for $\Delta V^{\neq}_{TST}$.

Bagchi and Oxtoby[24] have interpreted the slow decrease of the rate with solvent viscosity using the barrier dynamics expressions (54) and (56) and the observation that the solvent correlation time τ_c increases with the viscosity. As seen from Fig. 2 this also leads to a weak γ dependence of the rate. This is schematically illustrated by the dashed line in Fig. 2(a) which connects points which lie on higher τ_c curves for higher γ. The results of the present work indicate that within the one dimensional model considered not only the barrier dynamics but also the shape of the potential well (expressed here by the ratio ω_0/ω_B) affect the viscosity dependence of the rate.

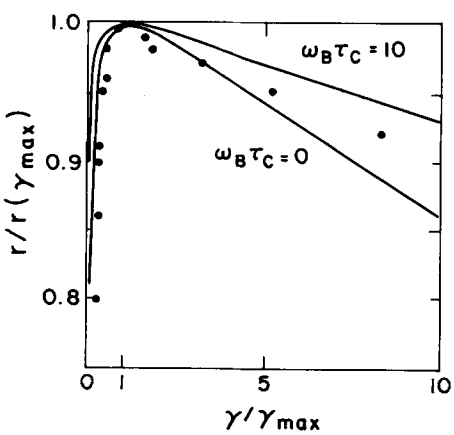

FIG. 4. r/r_{max} vs γ/γ_{max} for a symmetric double potential well with $E_B = 10.7$ kcal/mol and $\omega_0/\omega_B = 0.2$. The full lines are the theoretical results obtained for different values of the parameter $\omega_B\tau_C$. The points are the experimental results of Hasha *et al.* (Ref. 13) corresponding to $\Delta V^{\neq}_{TST} = -1.5$ cm^3/mol.

Finally, we note that we have tacitly assumed above that the zero frequency friction γ and the zero frequency viscosity η are linearly related. This seems to be approximately true in the range of viscosities used in the experimental studies. See Refs. 24 and 12(b) for further discussions of this point.

APPENDIX A

Here we outline the mathematical steps which lead to the results in Eq. (40).

Denoting

$$C_W = \int_{J_{0W}}^{J_{1W}} dJ \frac{\omega_W(J)}{\gamma J} \exp(E_W(J)/kT), \tag{A1}$$

we rewrite Eq. (24) in the form

$$A_{0W} = A_W(B_W + C_W), \tag{A2}$$

Eqs. (23), (27), (30), and (31) lead to

$$A_L B_L = \frac{2\pi}{M} F_2\left(F_1 + \int_0^{-\gamma(\alpha+1)X_{1L}} dz \exp\left(-\alpha\frac{Mz^2}{2kT}\right)\right), \tag{A3}$$

$$A_R B_R = \frac{2\pi}{M} F_2 e^{-\Delta E/kT}\left[F_1 + \int_0^{-\gamma(\alpha+1)X_{1R}} dz \exp\left(-\alpha\frac{Mz^2}{2kT}\right)\right]. \tag{A4}$$

Using Eqs. (28) and (33) these can be recast in the forms

$$A_L B_L = \frac{2\pi}{M} F_2\left(F_1 + \sqrt{\frac{\pi kT}{2\alpha M}} R_L\right), \tag{A5}$$

$$A_R B_R = \frac{2\pi}{M} F_2 e^{-\Delta E/kT}\left(F_1 - \sqrt{\frac{\pi kT}{2\alpha M}} R_R\right), \tag{A6}$$

where (erf is the error function)

$$R_W = \mathrm{erf}\sqrt{(\alpha+1)(E_{BW} - E_{1W})/kT}), \tag{A7}$$

Eqs. (26), (29), and (37) lead to

$$A_L = -A_R = \frac{F_2}{M^{3/2}}\sqrt{\frac{2\pi kT}{\alpha+1}} \exp\left(-\frac{E_{BL}}{kT}\right). \tag{A8}$$

Finally Eqs. (23), (27), (35), and (36) lead to equations for E_{1L} and E_{1R} (and thus for the associated X_{1L}, X_{1R}, and J_{1L}, J_{1R}). These are

$$\exp\left[-\alpha\frac{E_{BW} - E_{1W}}{kT}\right] = \sqrt{\alpha\frac{E_{BW} - E_{1W}}{kT}}\frac{kT}{\gamma J_{1W}\sqrt{\pi}(\alpha+1)}. \tag{A9}$$

In addition to these relations we have also [from Eqs. (38) and (A2)]

$$\frac{A_L(B_L + C_L)}{A_R(B_R + C_R)} = q_0\frac{\omega_{0L}}{\omega_{0R}}. \tag{A10}$$

To simplify the following discussion we may also use the fact that the final result is derived by dividing by a normalization factor. This enables us to choose one of the parameters A, B, or F at will. In what follows we use

$$A_L = -A_R = 1, \tag{A11}$$

Eqs. (A5), (A6), (A8), and (A10) can be now used to find the remaining parameters F_1, F_2, B_L, and B_R. They lead to

$$F_1 = \frac{1}{\bar{q}-1}\left\{\sqrt{\frac{\pi kT}{2\alpha M}}\,(R_L + \bar{q}R_R) + \sqrt{\frac{kT}{2\pi M(\alpha+1)}} \times\left[C_L \exp\left(-\frac{E_{BL}}{kT}\right) + \bar{q}C_R \exp\left(-\frac{E_{BR}}{kT}\right)\right]\right\}, \tag{A12}$$

where

$$\bar{q} = q_0 \frac{\omega_{0L}}{\omega_{0R}} e^{-\Delta E/kT}. \tag{A13}$$

In what follows it is convenient to use the following quantities:

$$Q_L = \int_{-\infty}^{0} dx \int_{-\infty}^{\infty} dv \exp\left\{-\left[\frac{M}{2}v^2 + V(x)\right]/kT\right\} \simeq \frac{2\pi}{M}\int_0^{\infty} \frac{dE}{\omega_L(E)} \exp\left(-\frac{E}{kT}\right) \simeq \frac{2\pi kT}{M\omega_{0L}}, \tag{A14}$$

$$Q_R = \int_{0}^{\infty} dx \int_{-\infty}^{\infty} dv \exp\left\{-\left[\frac{M}{2}v^2 + V(x)\right]/kT\right\} \simeq \frac{2\pi kT}{M\omega_{0R}} e^{-\Delta E/kT}. \tag{A15}$$

The quantity

$$q_e \equiv \frac{Q_L}{Q_R} = \frac{\omega_{0R}}{\omega_{0L}} e^{\Delta E/kT} \tag{A16}$$

is the equilibrium population ratio between the two wells, while q_0 defined by Eq. (38) is equal to $A_{0L}Q_L/A_{0R}Q_R$. Equation (A13) is equivalent to

$$\bar{q} = q_0/q_e. \tag{A17}$$

Next we calculate the steady state "populations"

$$N_L = \int_{-\infty}^{0} dx \int_{-\infty}^{\infty} dv\, P(x,v), \tag{A18}$$

$$N_R = \int_{0}^{\infty} dx \int_{-\infty}^{\infty} dv\, P(x,v). \tag{A19}$$

Each of these is calculated as a sum of three contributions corresponding to the $E<E_1$; $E>E_1$, $x>X_1$ *and* $E>E_1$, $x<X_1$ regions of phase space associated with each well. This calculation follows the same steps of a similar calculation described for the single well model and yields

$$N_L = kT\tau_L + F_1F_2Q_L + F_2\sqrt{\frac{\pi kT}{2M\alpha}}\,S_L, \tag{A20}$$

$$N_R = kT\tau_R + F_1F_2Q_R - F_2\sqrt{\frac{\pi kT}{2M\alpha}}\,S_R, \tag{A21}$$

where

$$S_L = \frac{2\pi}{M}\int_0^{E_{BL}} \frac{dE}{\omega_L(E)}[\eta(E-E_{1L}) + R_L\eta(E_{1L}-E)] \times \exp(-E/kT), \tag{A22}$$

$$S_R = \frac{2\pi}{M} e^{-\Delta E/kT} \times \int_0^{E_{BR}} \frac{dE}{\omega_R(E)}[\eta(E-E_{1R}) + R_R\eta(E_{1R}-E)] \times \exp(-E/kT), \tag{A23}$$

$$\eta(x) = \begin{cases} 0, & x<0, \\ 1, & x>0, \end{cases} \tag{A24}$$

and where

$$\tau_W = \frac{1}{kT}\int_{J_{0W}}^{J_{1W}} dJ \frac{\omega_W(J)}{\gamma J} \exp\left[\frac{E_W(J)}{kT}\right] \int_0^{J} dJ' \times \exp\left[-\frac{E_W(J)}{kT}\right] \quad (W = L, R), \tag{A25}$$

τ_W $(W = L, R)$ are the mean first passage times to reach J_{1W} from J_{0W}, given a reflecting barrier at $J_W = 0$.

The normalized current r [Eq. (39) with $N = N_L + N_R$] is obtained using Eqs. (26), (A11), (A20), and (A21). The result is

$$r = \frac{kT}{kT(\tau_L - \tau_R) + g_1(S_L - S_R) + g_2\left[g_1(R_L + g_3R_R) + \frac{M}{2\pi}(C_L + g_4C_R)\right]}, \tag{A26}$$

$$g_1 = \frac{M}{2}\sqrt{\frac{\alpha+1}{\alpha}} \exp(E_{BL}/kT), \tag{A27}$$

$$g_2 = (Q_L + Q_R)/(g_3 - 1), \tag{A28}$$

$$g_3 = g_4 \exp\left(-\frac{\Delta E}{kT}\right), \tag{A29a}$$

$$g_4 = q_0\omega_{0L}/\omega_{0R}. \tag{A29b}$$

Note that r in Eq. (A26) is defined to be positive for a net current from left to right. This cumbersome (but straightforward to calculate) expression for r may be cast in the more transparent form

$$r = \frac{q_s - q_e}{q_s + 1}\left[\tau_L + q_e\tau_R + \tfrac{1}{2}(\bar{S}_L + \bar{S}_R)r_{K,RL}^{-1}\right]^{-1}, \tag{A30}$$

where

$$q_s \equiv N_L/N_R \tag{A31}$$

is the steady state population ratio,

$$r_{K,RL} = \frac{\omega_{0L}}{2\pi\omega_B}\left[\sqrt{\left(\frac{\gamma}{2}\right)^2 + \omega_B^2} - \frac{\gamma}{2}\right]\exp\left(-\frac{E_{BL}}{kT}\right) \tag{A32}$$

is the Kramers' left to right rate for a single well model, and where

$$\bar{S}_L = S_L/Q_L; \quad \bar{S}_R = S_R/Q_R \,. \tag{A33}$$

Putting all the population on the left ($q_s \to \infty$)[23] we obtain the left to right steady state rate

$$r_{RL} = r(q_s \to \infty) = \left[\tau_L + q_e\tau_R + \tfrac{1}{2}(\bar{S}_L + \bar{S}_R)r_{K,RL}^{-1}\right]^{-1}. \tag{A34}$$

Similarly the right to left rate is

$$r_{LR} = -r(q_s \to 0) = q_e r_{RL}$$
$$= \left[\frac{1}{q_e}\tau_L + \tau_R + \tfrac{1}{2}(\bar{S}_L + \bar{S}_R)r_{K,LR}^{-1}\right]^{-1} \tag{A35}$$

with the right to left Kramers' single well rate

$$r_{K,LR} = \frac{\omega_{0R}}{2\pi\omega_B}\left[\sqrt{\left(\frac{\gamma}{2}\right)^2 + \omega_B^2} - \frac{\gamma}{2}\right]\exp\left(-\frac{E_{BR}}{kT}\right). \tag{A36}$$

[1] B. Carmeli and A. Nitzan, Phys. Rev. Lett. **49**, 423 (1982); J. Chem. Phys. **79**, 393 (1983); Isr. J. Chem. **22**, 360 (1982).

[2] B. Carmeli and A. Nitzan, Phys. Rev. A (in press); Phys. Rev. Lett. **51**, 233 (1983).

[3] H. A. Kramers, Physica (Ultrecht) **7**, 284 (1940).

[4] (a) R. F. Grote and J. T. Hynes, J. Chem. Phys. **73**, 2715 (1980); (b) **74**, 4465 (1981); (c) **77**, 3736 (1982).

[5] P. Hanggi and F. Mojtabai, Phys. Rev. A **26**, 1168 (1982); J. Stat. Phys. **30**, 401 (1983).

[6] (a) D. Chandler, J. Chem. Phys. **68**, 2959 (1978); (b) J. A. Montgomery, D. Chandler, and B. J. Berne, *ibid.* **70**, 4056 (1979); (c) J. A. Montgomery, S. L. Holmgren, and D. Chandler, *ibid.* **73**, 3688 (1980).

[7] (a) S. H. Northrup and J. T. Hynes, J. Chem. Phys. **69**, 5246 (1978); (b) **73**, 2700 (1980).

[8] J. L. Skinner and P. G. Wolynes, J. Chem. Phys. **69**, 2143 (1978); **72**, 4913 (1980).

[9] D. K. Garrity and J. L. Skinner, Chem. Phys. Lett. **95**, 46 (1983).

[10] R. S. Larson and M. D. Kostin, J. Chem. Phys. **72**, 1392 (1980).

[11] (a) N. G. Van Kampen, J. Stat. Phys. **17**, 71 (1977); (b) E. Helfand, J. Chem. Phys. **69**, 1010 (1978); (c) N. De Leon and B. J. Berne, *ibid.* **75**, 3495 (1981); (d) K. Shultan, Z. Shultan and A. Szabo, *ibid.* **74**, 4426 (1981); (e) L. E. Reichl, *ibid.* **77**, 4199 (1982); (f) B. J. Matkowsky, Z. Scshuss, and E. Ben-Jacob, SIAM J. Appl. Math. **42**, 835 (1982); (g) M. O. Hongler and W. M. Zheng, J. Stat. Phys. **29**, 317 (1982); (h) C. W. Gardiner, *ibid.* **30**, 157 (1983).

[12] (a) S. P. Velsko and G. R. Fleming, Chem. Phys. **65**, 59 (1982); J. Chem. Phys. **76**, 3553 (1982); (b) S. P. Velsko, D. H. Waldek, and G. R. Fleming, J. Chem. Phys. **78**, 249 (1983).

[13] D. L. Hasha, T. Eguchi, and J. Jonas, J. Am. Chem. Soc. **104**, 2290 (1982); J. Chem. Phys. **75**, 1570 (1981).

[14] B. I. Greene, R. M. Hochstrasser, and R. B. Weisman, Chem. Phys. Lett. **62**, 427 (1979); Chem. Phys. **48**, 289 (1980).

[15] (a) J. R. Taylor, M. C. Adams, and W. Sibbett, Appl. Phys. Lett. **35**, 590 (1979); (b) I. Glatt and A. Yogev, Chem. Phys. Lett. **77**, 228 (1981); (c) D. C. Knauss and G. T. Evans, J. Chem. Phys. **74**, 4627 (1981); (d) J. Buechele, E. Weitz, and F. D. Lewis, *ibid.* **77**, 3500 (1982).

[16] The frequencies ω_{0L} and ω_{0R} appear in the theory by making approximations of the form $\int_0^{E_{BW}} dE\omega_W(E)^{-1}\exp(-E/kT) \cong kT/\omega_{0W}$ ($W = L, R$). Alternatively one can use this relation as a definition of ω_{0W}.

[17] S. A. Adelman, J. Chem. Phys. **64**, 124 (1976).

[18] In Ref. 2 we have shown in a model calculation that for $E_B = 10kT$ changing E_0 between 0 and 1/2 E_B makes an effect of $<1\%$. For $E_B = 4kT$ the effect is of order $\sim 5\%$.

[19] This population ratio is $= A_{0L}\int dJ\, e^{-E_L(J)/kT}/A_{0R}\int dJ e^{-E_R(J)/kT}$ which leads to the result in the text by moving ω_{0L} and ω_{0R} out of the integrals (see Ref. 16).

[20] Equation (60) is obtained from Eq. (44) by replacing in the first integral the coefficient of $\exp(E_W/kT)$ by its value of $J = J_{1W}$ and by writing for the second integral kT/ω_{0W} (see also Ref. 16). The usual Kramers expression for the single well escape rate in the low friction limit is obtained from the inverse τ_W^{-1} of Eq. (60) by replacing E_{1W} and J_{1W} by E_{1W} and J_{1B} and by identifying $\omega_0 J_B$ with E_B for the truncated harmonic oscillator model.

[21] In Ref. 2 we have denoted $1/2\,(S_L + 1)$ by S.

[22] In Ref. 6 thermal interactions are taken into account using the impact collision model.

[23] Note that at steady state q_s is finite (even though the initial population ratio q_0 may be 0 or ∞). For deep wells it is physically obvious and may be mathematically shown that if q_0 is 0 or ∞ than $q_s < q_e$, 1 or $q_s > q_e$, 1 respectively.

[24] B. Bagchi and D. W. Oxtoby, J. Chem. Phys. **78**, 2735 (1983).

[25] It should be pointed out that Garrity and Skinner (Ref. 9) use not the Markovian Langevin equations (3) and (4) but, following Skinner and Wollynes (Ref. 8), the BGK collision model in which individual collisions with the solvent molecules can cause large changes in the kinetic energy. Comparing our numerical results with those of Ref. 9, it is seen that for highly averaged quantities like the escape rate from relatively deep wells the two models yield qualitatively similar results.